

AN ASYMPTOTIC SOLUTION FOR LARGE PRANDTL NUMBER FREE CONVECTION

H. K. Kuiken*

Technological University of Delft, Department of Mathematics

SUMMARY

The set of ordinary differential equations governing free convection boundary layer flow past an isothermal semi-infinite vertical flat plate is solved for large Prandtl numbers by means of the method of matched asymptotic expansions. The analysis leads to an expression for heat transfer which contains the Prandtl number explicitly and which is very accurate for sufficiently large values of the Prandtl number. On the other hand the analysis also has qualitative assets. Before choosing the mathematical method of solution, the physical aspects of the large Prandtl number free convection boundary layer are investigated. The mathematical solution serves to enlarge our understanding of the physical implications of a free convection boundary layer in a large Prandtl number fluid.

NOMENCLATURE

- a_{ij} coefficient defined by $\lim_{\eta \rightarrow \infty} f_j = a_{0j} + a_{1j}\eta + a_{2j}\eta^2 + \dots$
 b_{ij} coefficient defined by $F_j(\xi) = b_{0j} + b_{1j}\xi + b_{2j}\xi^2 + \dots$
 c coefficient defined by equation (3)
 c_p specific heat
 f non-dimensional stream function of inner expansion (7)
 f_n n-th perturbation of f
 F non-dimensional stream function of outer expansion (15)
 g non-dimensional stream function (1)
 \bar{g} acceleration due to gravity
 Gr_x local Grashof number: $g\beta(T_w - T_\infty)x^3/\nu^2$
 h non-dimensional temperature (2)
 k coefficient of heat conduction
 Nu_x local Nusselt number: $-\frac{x}{T_w - T_\infty} \frac{\partial T}{\partial y} \Big|_{y=0}$
 T temperature
 T_w wall-temperature
 T_∞ ambient temperature
 u longitudinal velocity
 x co-ordinate measuring distance from the leading edge
 y co-ordinate measuring distance normal to the plate

Greek symbols

β coefficient of thermal expansion

* Present address: University of British Columbia, Department of Mechanical Engineering, Vancouver

- δ_i expansion parameter (21)
 $\bar{\delta}_i$ expansion parameter (22)
 Δ_i expansion parameter (33)
 $\bar{\Delta}_i$ expansion parameter (34)
 ϵ expansion parameter: $\sigma^{-\frac{1}{2}}$
 η inner similarity co-ordinate (9)
 θ non-dimensional temperature of inner expansion (8)
 θ_n n-th perturbation of θ
 \mathcal{D} non-dimensional temperature of outer expansion (16)
 \mathcal{D}_n n-th perturbation of \mathcal{D}
 μ similarity co-ordinate (3)
 ν kinematic viscosity
 ξ outer similarity co-ordinate (17)
 ρ density
 σ Prandtl number: $\frac{\nu \rho c_p}{k}$
 ψ stream function

1. Introduction

It is well-known that in heat transfer through viscous fluid flows the Prandtl number σ plays a very important role. Mathematically this role is generally expressed through the occurrence of this number in the governing non-dimensional partial differential equations. While for moderate values of σ the integration of these equations can be performed easily - that is to say for relatively simple problems - the extreme values ($\sigma \sim 0$, $\sigma \rightarrow \infty$) have proved to be sources of trouble. For these extreme values of the Prandtl number the boundary layer of free convection approaches a singular character so that a direct regular perturbation technique cannot be applied for obtaining insight in free convection under such conditions.

The first paper unveiling some of the intricacies of this matter is the work of Le Fevre [1]. In earlier papers of Schuh [2] and Ostrach [3] the equations were integrated for particular small or large Prandtl numbers by means of a computer. Although these integrations give valuable qualitative information, e.g. about the ratio of the thicknesses of the velocity- and the temperature boundary layer in the limiting cases, a more satisfactory analysis will involve a singular perturbation technique having $\sigma=0$ or $\sigma=\infty$ as zeroth perturbation. In his analysis Le Fevre has tried to furnish these limiting cases but he only achieved a partial success. As the limiting case of small σ he saw the inviscid free convection boundary layer. It is impossible, however, to describe small Prandtl number free convection by perturbing inviscid free convection directly. Recently Kuiken [4] has solved this problem by stating that σ can also approach zero if $k \rightarrow \infty$. In this case the limiting character of the free convection boundary layer is a viscous boundary layer of forced flow type. Lykoudis [5] was the first to recognize this behavior of the inner part of the free convection boundary layer. Using this boundary layer as the main term of an inner expansion and Le Fevre's inviscid layer as the zeroth perturbation of an outer expansion it was shown that this problem could be solved by the method of matched asymptotic expansions.

It has also been shown by the present author [4, 15] that the same dual character of free convection boundary layer flow exists for $\sigma \rightarrow \infty$. This problem, however, was not solved explicitly. It is the purpose of this paper

to fill this gap. It has to be mentioned that the method of matched asymptotic expansions has been applied already to forced convection at large σ [6]. Forced convection, however, is relatively simple since the momentum- and energy equation are uncoupled. In free convection the temperature- and velocity effects are completely interwoven so that the understanding and description of the physical implications is a more complicated task than it is for forced flow especially under extreme Prandtl number conditions. Consequently it is necessary to carefully present an analysis of the physical picture of free convection at large σ . When once the physical background is totally understood the way to the mathematical solution is easy to find. Finally we may remark that approximate solutions for large Prandtl number free convection have been found by several authors. We may mention the work of Morgan and Warner [7] whose analysis is virtually the same as Le Fevre's. They tried to extend their results to some larger Prandtl number range. The method of steepest descent as introduced in the theory of boundary layers by Meksyn [8] and Merk [9] has been applied to free convection by Brindley [10]. Braun and Heighway [11] developed an integral method for both very small and very large Prandtl numbers.

2. Physical analysis of the boundary layer.

Although it is possible to derive the physical picture of large Prandtl number free convection by pure physical contemplation, it seems to be expedient and might enhance our chances of a successful investigation to use the mathematical achievements given in the literature. Let us consider therefore the Figs. 1 and 2 where the temperature and velocity profiles, as cal-

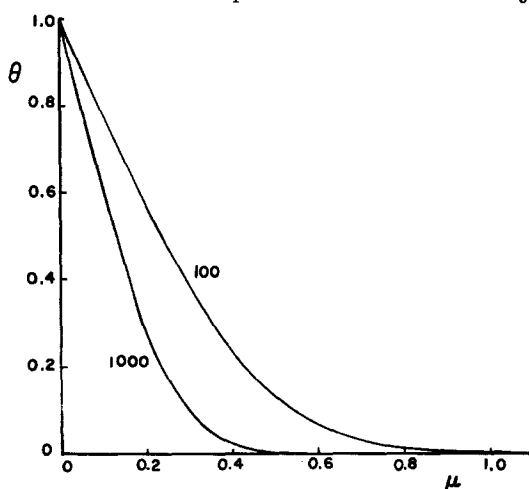


Fig. 1 Temperature profiles for $\sigma = 100$ and $\sigma = 1000$ (Ostrach [3])

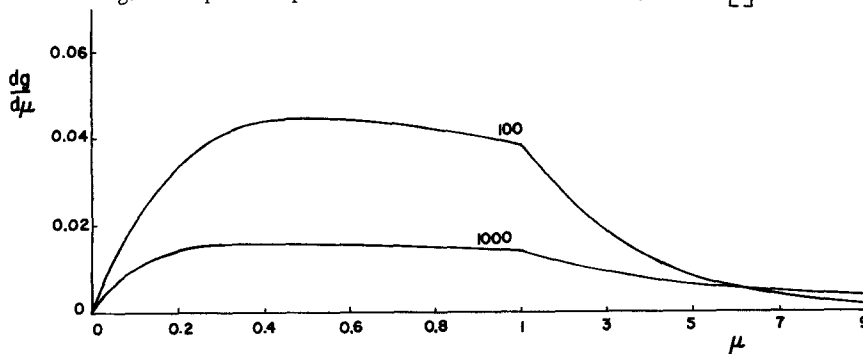


Fig. 2 Velocity profiles for $\sigma = 100$ and $\sigma = 1000$ (Ostrach [3])

culated by Ostrach [3] for $\sigma=100$ and $\sigma=1000$, have been given. These graphs clearly show features about which the following remarks may be made:

- 1° the temperature boundary layer is very thin,
- 2° although the velocity is small the velocity boundary layer is much thicker than the temperature boundary layer,
- 3° in the temperature boundary layer the velocity grows rapidly and reaches its maximum value near the outer edge of the temperature boundary layer,
- 4° outside the temperature boundary layer the velocity decreases slowly to zero,
- 5° the effects 1° through 4° are more pronounced for large σ .

These remarks undoubtedly demonstrate that for large Prandtl numbers the free convection boundary layer consists of two regions where different phenomena are predominant. First, there is an inner region where tangible temperature differences with the ambient fluid exist. Only in this region there are buoyancy effects. Consequently in this region the transport terms and the conduction terms of the energy equation have to be of the same order of magnitude. Moreover, as a large Prandtl number fluid can be considered to be very viscous the buoyancy term has to be of the same order of magnitude as the viscous term. This decision is quite realistic since, as we have remarked in 3°, the velocity gradients and thus the viscous stresses are large in the temperature boundary layer. Second, we have an outer region where no buoyancy exists. The fluid in this region is flowing due to viscous contact with the inner region. In the extreme case ($\sigma \rightarrow \infty$) this layer might be described as a viscous boundary layer of forced flow type the force being exerted at the flat plate due to buoyancy. It is clear that the equations for this layer may be derived by imposing two conditions. First, the longitudinal velocity has to be of the same order of magnitude as the corresponding velocity in the inner layer. Second, the inertia terms and the viscous terms have to be of the same order of magnitude (condition of Prandtl for forced boundary layer [12]).

3. *Mathematical analysis of the boundary layer.*

Guided by the physical conclusions just presented we will endeavor to develop exact numerical results for large Prandtl number free convection. If we restrict ourselves to the vertical flat plate having a uniform temperature T_w it is a known fact [3] that through substitution of

$$\psi = 4 \nu c x^{\frac{3}{4}} g(\mu), \quad (1)$$

$$T = T_{\infty} + (T_w - T_{\infty}) h(\mu), \quad (2)$$

$$\mu = c y x^{-\frac{1}{4}}; \quad c = \left\{ \frac{\bar{g} \beta (T_w - T_{\infty})}{4 \nu^2} \right\}^{\frac{1}{4}} \quad (3)$$

in the momentum- and energy equation the following set of ordinary differential equations is obtained

$$\frac{d^3 g}{d\mu^3} + 3g \frac{d^2 g}{d\mu^2} - 2 \left(\frac{dg}{d\mu} \right)^2 + h = 0, \quad (4)$$

$$\frac{d^2 h}{d\mu^2} + 3\sigma g \frac{dh}{d\mu} = 0. \tag{5}$$

For later use it is also necessary to present the expression for the longitudinal velocity

$$u = \frac{\partial \psi}{\partial y} = 4\nu c^2 x^{\frac{1}{2}} \frac{dg}{d\mu}. \tag{6}$$

the inner problem

First we will try to describe the layer nearest to the wall, which is the temperature boundary layer. For obvious reasons this layer will be called the inner region. Let us consider a transformation of variables

$$g = \sigma^{-\frac{3}{4}} f(\eta), \tag{7}$$

$$h = \theta(\eta), \tag{8}$$

$$\mu = \eta \sigma^{-\frac{1}{4}}. \tag{9}$$

The resulting momentum- and energy equation are

$$\frac{d^3 f}{d\eta^3} + \theta + \epsilon^2 \left\{ 3f \frac{d^2 f}{d\eta^2} - 2 \left(\frac{df}{d\eta} \right)^2 \right\} = 0, \tag{10}$$

$$\frac{d^2 \theta}{d\eta^2} + 3f \frac{d\theta}{d\eta} = 0, \tag{11}$$

with $\epsilon = \sigma^{-\frac{1}{2}}$. These equations clearly satisfy the conditions imposed upon the inner region, i.e. the conduction- and convection terms are of equal order of magnitude in the energy equation and in the momentum equation this is true for the viscous- and the bouyancy terms. Furthermore we have

$$\psi_{\text{inner}} = 4\nu c x^{\frac{3}{4}} \epsilon^{\frac{3}{2}} f(\eta), \tag{12}$$

$$T_{\text{inner}} = T_{\infty} + (T_w - T_{\infty}) \theta(\eta), \tag{13}$$

$$U_{\text{inner}} = 4\nu c^2 x^{\frac{1}{2}} \epsilon \frac{df}{d\eta}. \tag{14}$$

the outer problem

By substitution of

$$g = \sigma^{-\frac{1}{4}} F(\xi), \tag{15}$$

$$h = \mathcal{V}(\xi), \tag{16}$$

$$\mu = \xi \sigma^{\frac{1}{4}}, \tag{17}$$

in the equations (4) and (5) we obtain

$$\frac{d^3 F}{d\xi^3} + 3F \frac{d^2 F}{d\xi^2} - 2 \left(\frac{dF}{d\xi} \right)^2 + \epsilon^{-2} \mathcal{V} = 0, \tag{18}$$

$$3F \frac{d\vartheta}{d\xi} + \epsilon^2 \frac{d^2\vartheta}{d\xi^2} = 0. \tag{19}$$

Since the longitudinal velocity appears to be

$$U_{\text{outer}} = 4\nu c^2 x^{\frac{1}{2}} \epsilon \frac{dF}{d\xi}, \tag{20}$$

it becomes clear upon comparing (14) and (20) that u is of the same order of magnitude in both layers. Moreover, the viscous- and inertia terms in the momentum equation (18) are, as required, of the same order of magnitude. At first sight it seems, however, somewhat contradictory in equation (18) that the buoyancy term is multiplied by the large parameter ϵ^{-2} . Buoyancy was thought to play a minor role in the outer layer. This problem can be solved very soon by considering equation (19). If we insert in this equation expansions of the following type

$$F(\xi) = F_0(\xi) + \delta_1(\epsilon) F_1(\xi) + \delta_2(\epsilon) F_2(\xi) + \dots, \tag{21}$$

$$\vartheta(\xi) = \vartheta_0(\xi) + \bar{\delta}_1(\epsilon) \vartheta_1(\xi) + \bar{\delta}_2(\epsilon) \vartheta_2(\xi) + \dots \tag{22}$$

with

$$\lim_{\epsilon \rightarrow 0} \frac{\delta_{i+1}}{\delta_i} = 0; \quad \lim_{\epsilon \rightarrow 0} \frac{\bar{\delta}_{i+1}}{\bar{\delta}_i} = 0; \quad \delta_0 = \bar{\delta}_0 = 1, \tag{23}$$

then the zeroth perturbation yields

$$F_0 \frac{d\vartheta_0}{d\xi} = 0. \tag{24}$$

We have to rule out $F_0=0$ as a solution since F is connected with the stream function which is always positive, save at the wall. Hence $d\vartheta_0/d\xi=0$ yielding $\vartheta_0=\text{constant}$. This constant has to be zero since $\vartheta(\infty)=0$. Hence $\vartheta_0=0$. For the first perturbation we now have the equation

$$F_0 \frac{d\vartheta_1}{d\xi} = 0. \tag{25}$$

For similar reasons as were advanced for ϑ_0 we infer $\vartheta_1=0$. It immediately follows now that all perturbations of the temperature are zero in the outer region. As a consequence we are left with one equation for the description of the outer layer.

$$\frac{d^3F}{d\xi^3} + 3F \frac{d^2F}{d\xi^2} - 2 \left(\frac{dF}{d\xi} \right)^2 = 0. \tag{26}$$

This result is in complete agreement with what we already remarked about the character of the outer layer. It is a layer of forced flow type the force being exerted at the wall through buoyancy. The mathematical translation of these physical remarks is that according to the well-known matching principle [13] the outer layer has to be brought into contact with the inner layer which is the layer of the buoyancy forces. With respect to this it is interesting to remark that the analysis of forced flow along a moving flat plate with a spatially varying velocity distribution proportional to

$x^{\frac{1}{2}}$ will lead to equation (26) if an appropriate similarity transformation is applied. The occurrence of the coefficient $x^{\frac{1}{2}}$ in (6), (14) and (20) is in logical agreement with this.

For matching purposes the expression

$$\psi_{\text{outer}} = 4 \nu c x^{\frac{3}{4}} \epsilon^{\frac{1}{2}} F(\xi) = 4 \nu c x^{\frac{3}{4}} \epsilon^{\frac{1}{2}} F(\eta\epsilon) \tag{27}$$

will prove to be most useful.

matching

The boundary conditions which the various functions have to satisfy can partly be derived from the original boundary conditions imposed upon the original functions $g(\mu)$ and $h(\mu)$. That is to say the inner boundary conditions have to be allotted to the inner problem while the outer functions have to satisfy the ambient conditions. We consequently have

$$f = 0, \quad \frac{df}{d\eta} = 0, \quad \theta = 1 \quad \text{at} \quad \eta = 0, \tag{28}$$

$$\frac{dF}{d\xi} \rightarrow 0 \quad \text{as} \quad \xi \rightarrow \infty. \tag{29}$$

It is quite clear that additional boundary conditions have to be found for $\eta \rightarrow \infty$ and for $\xi \downarrow 0$. Here the matching principle enters the problem. It is most easily applied to the temperature. On account of the fact that for the outer problem the temperature is exactly equal to zero we may immediately infer

$$\theta \rightarrow 0 \quad \text{as} \quad \eta \rightarrow \infty. \tag{30}$$

For the matching of the inner- and outer stream function ψ_{inner} and ψ_{outer} a full-fledged matching formula has to be presented

$$\lim_{\eta \rightarrow \infty} \psi_{\text{inner}} = \lim_{\xi \downarrow 0} \psi_{\text{outer}}, \tag{31}$$

which on using (12) and (27) leads to

$$\lim_{\eta \rightarrow \infty} \epsilon f(\eta) = \lim_{\xi \downarrow 0} F(\eta\epsilon). \tag{32}$$

With \lim we denote the behavior of a function in the direction given in the formula. Formula (32) provides both the outer boundary conditions for $f(\eta)$ and the inner boundary conditions of the outer problem.

4. *Solution*

zeroth perturbations

In (21) we already have given a series as a possible representation of the solution of the outer problem. For the inner problem we accordingly introduce

$$f(\eta) = f_0(\eta) + \Delta_1(\epsilon) f_1(\eta) + \Delta_2(\epsilon) f_2(\eta) + \dots \tag{33}$$

$$\theta(\eta) = \theta_0(\eta) + \bar{\Delta}_1(\epsilon) \theta_1(\eta) + \bar{\Delta}_2(\epsilon) \theta_2(\eta) + \dots \tag{34}$$

with

$$\lim_{\epsilon \rightarrow 0} \frac{\Delta_{i+1}}{\Delta_i} = 0; \quad \lim_{\epsilon \rightarrow 0} \frac{\bar{\Delta}_{i+1}}{\bar{\Delta}_i} = 0; \quad \Delta_0 = \bar{\Delta}_0 = 1. \tag{35}$$

The differential equations for the zeroth perturbations become upon substitution of (33), (34) and (21) in (10), (11) and (26)

$$\frac{d^3 f_0}{d\eta^3} + \theta_0 = 0, \tag{36}$$

$$\frac{d^2 \theta_0}{d\eta^2} + 3 f_0 \frac{d\theta_0}{d\eta} = 0, \tag{37}$$

$$\frac{d^3 F_0}{d\xi^3} + 3 F_0 \frac{d^2 F_0}{d\xi^2} - 2 \left(\frac{dF_0}{d\xi} \right)^2 = 0. \tag{38}$$

At this point it is necessary to recall that the asymptotic ($\eta \rightarrow \infty$) behavior of boundary layer solutions generally gives for the stream function a polynomial in η plus terms of exponentially small order (exp-). For example Blasius's solution gives for $\eta \rightarrow \infty$: $f \sim \eta + \text{constant} + \text{exp-}$ [14]. Without further proof and guided by this usual behavior we directly derive from equation (36) using the condition $\theta_0(\eta) \rightarrow 0$ as $\eta \rightarrow \infty$

$$\lim_{\eta \rightarrow \infty} f_0(\eta) \sim a_{20} \eta^2 + a_{10} \eta + a_{00} + \text{exp-}. \tag{39}$$

On writing

$$\lim_{\xi \downarrow 0} F_0(\xi) = b_{00} + b_{10} \xi + b_{20} \xi^2 + \dots \tag{40}$$

an evaluation of (32) up to terms of $O(\epsilon)$ gives

$$\epsilon(a_{20} \eta^2 + a_{10} \eta + a_{00}) = b_{00} + b_{10} \eta \epsilon. \tag{41}$$

Three results can be drawn at once from equation (41). First $b_{00} = 0$ which is equivalent with

$$F_0(0) = 0. \tag{42}$$

This condition is quite logical as it expresses that ψ_{outer} is zero at the wall for the extreme case $\sigma \rightarrow \infty$.

As a second result the comparison of left- and righthand side of (41) gives $a_{20} = 0$ or

$$\frac{d^2 f_0}{d\eta^2} \rightarrow 0 \quad \text{as} \quad \eta \rightarrow \infty. \tag{43}$$

This result we indeed may derive from (41) since a term with η^2 can only enter the righthand side of (41) through ξ^2 . Since $\xi = \eta \epsilon$ such a term can only occur in terms of $O(\epsilon^2)$ or higher orders. The third result to be obtained from (41) naturally is $b_{10} = a_{10}$ or

$$\left. \frac{df_0}{d\eta} \right|_{\eta \rightarrow \infty} = \left. \frac{dF_0}{d\xi} \right|_{\xi=0}. \tag{44}$$

This obviously is a matching of the longitudinal velocities which is the cause of the existence of the outer layer.

The system of equations (36) and (37) with the boundary conditions (28), (30) and (43) has already been found by Le Fevre [1] in his analysis of free convection for $\sigma \rightarrow \infty$. This author, however, did not give a reason for the introduction of condition (43). He did not include in his analysis, what we have called here, the outer layer. It must have become clear that only through using this layer one can deduce (43).

An integration of the equations of the zeroth inner perturbation with the appropriate boundary conditions gives

$$\lim_{\eta \rightarrow \infty} f_0(\eta) \sim 0.5106804 \eta - 0.261009 + \exp-. \tag{45}$$

Through (44) and (45) we may conclude

$$\left. \frac{dF_0}{d\xi} \right|_{\xi=0} = 0.5106804. \tag{46}$$

Integration of (38) with (29), (42) and (46) renders

$$\left. \frac{d^2 F_0}{d\xi^2} \right|_{\xi=0} = -0.5622789 = 2b_{20}. \tag{47}$$

With (42), (46) and (47) all subsequent coefficients of the series (40), representing a solution of F_0 for small values of ξ , can be calculated. These coefficients have to be available for matching of the higher perturbations.

first perturbations

We have now arrived at the question as to what should be the expansion variables $\Delta_1(\epsilon)$, $\bar{\Delta}_1(\epsilon)$ and $\delta_1(\epsilon)$ in (33), (34) and (21). If we assume as a representation of $F_n(\xi)$ near $\xi=0$

$$F_n(\xi) = b_{0n} + b_{1n}\xi + b_{2n}\xi^2 + \dots, \tag{48}$$

it is understood that the term $a_{00}\epsilon$ in the lefthand side of (41) can be produced by the righthand side by taking $\delta_1(\epsilon)=\epsilon$. Indeed, application of the matching rule (32) yields $b_{01}=a_{00}$ which on using (45) leads to

$$F_1(0) = -0.261009. \tag{49}$$

As the righthand side of (32) produces terms with ϵ^2 , ϵ^3 etc. we also decide that the expansion parameters $\Delta_1(\epsilon)$ and $\bar{\Delta}_1(\epsilon)$ are both equal to ϵ . Substitution of the expansions for f , θ and F in the corresponding equations gives for the equations of the first perturbations

$$\frac{d^3 f_1}{d\eta^3} + \theta_1 = 0, \tag{50}$$

$$\frac{d^2 \theta_1}{d\eta^2} + 3f_0 \frac{d\theta_1}{d\eta} + 3f_1 \frac{d\theta_0}{d\eta} = 0, \tag{51}$$

$$\frac{d^3 F_1}{d\xi^3} + 3F_0 \frac{d^2 F_1}{d\xi^2} - 4 \frac{dF_0}{d\xi} \frac{dF_1}{d\xi} + 3 \frac{d^2 F_0}{d\xi^2} F_1 = 0. \tag{52}$$

Application of (30) and (50) yields

$$\frac{d^3 f_1}{d\eta^3} \rightarrow 0 \quad \text{as } \eta \rightarrow \infty \tag{53}$$

or

$$\lim_{\eta \rightarrow \infty} f_1(\eta) = a_{21}\eta^2 + a_{11}\eta + a_{01} + \exp-. \tag{54}$$

On writing down (32) for terms of $O(\epsilon^2)$ we obtain

$$\epsilon^2(a_{21}\eta^2 + a_{11}\eta + a_{01}) = \epsilon^2(b_{20}\eta^2 + b_{11}\eta + \dots). \tag{55}$$

Obviously $a_{21}=b_{20}$ or using (47) and (54)

$$\frac{d^2 f_1}{d\eta^2} \rightarrow -0.5622789 \quad \text{as } \eta \rightarrow \infty. \tag{56}$$

With (30), (56) and the inner conditions $f_1=0, df_1/d\eta=0, \theta_1=0$ at $\eta=0$ the equations (50) and (51) can be integrated. For (54) we now find

$$\lim_{\eta \rightarrow \infty} f_1(\eta) = -0.2811394\eta^2 + 0.338836\eta - 0.27605 + \exp -. \tag{57}$$

On deriving $a_{11}=b_{11}$ from (55) we find using (48), (54) and (57) the remaining boundary condition for the outer problem

$$\left. \frac{dF_1}{d\xi} \right|_{\xi=0} = 0.338836. \tag{58}$$

With (29), (49) and (58) we can integrate (52). For matching purposes we give here

$$\left. \frac{d^2 F_1}{d\xi^2} \right|_{\xi=0} = -0.351566 = 2b_{21} \tag{59}$$

higher perturbations

In order to obtain results which are of a high degree of accuracy for a considerable Prandtl number range it is justified to give the second perturbations. Without going into much detail now it suffices to remark that it is easy to prove that the expansion variables $\Delta_2(\epsilon), \bar{\Delta}_2(\epsilon)$ and $\delta_2(\epsilon)$ are all equal to ϵ^2 . The resulting equations are

$$\frac{d^3 f_2}{d\eta^3} + \theta_2 + 3f_0 \frac{d^2 f_0}{d\eta^2} - 2 \left(\frac{df_0}{d\eta} \right)^2 = 0, \tag{60}$$

$$\frac{d^2 \theta_2}{d\eta^2} + 3f_0 \frac{d\theta_2}{d\eta} + 3 \frac{d\theta_0}{d\eta} f_2 + 3f_1 \frac{d\theta_1}{d\eta} = 0, \tag{61}$$

$$\frac{d^3 F_2}{d\xi^3} + 3F_0 \frac{d^2 F_2}{d\xi^2} - 4 \frac{dF_0}{d\xi} \frac{dF_1}{d\xi} + 3 \frac{d^2 F_0}{d\xi^2} F_2 +$$

$$+ 3 F_1 \frac{d^2 F_1}{d\xi^2} - 2 \left(\frac{dF_1}{d\xi} \right)^2 = 0. \tag{62}$$

If we search first for the outer boundary conditions of the inner problem we have to write down the coefficient of ϵ^3 of the righthand side of (32). This given

$$\lim_{\eta \rightarrow \infty} f_2(\eta) = b_{30} \eta^3 + b_{21} \eta^2 + b_{12} \eta + b_{03} + \text{exp-}. \tag{63}$$

In (63) both b_{30} and b_{21} (see(59)) are known. That f_2 can indeed satisfy a behavior as presented in (63) can immediately be seen by considering equation (60) for large values of η and neglecting exp-. From (45) and (60) follows

$$\frac{d^3 f_2}{d\eta^3} \rightarrow 2(0.510680)^2 = 0.521589 \tag{64}$$

so that

$$f_2 \rightarrow 0.086931 \eta^3 + \text{terms of order lower } \eta^3. \tag{65}$$

By substitution of (40) in (38) one can immediately verify that the coefficients of η^3 in (63) and (65) coincide. We accordingly have to integrate (60) and (61) with the condition that the coefficient of η^2 in $\lim_{\eta \rightarrow \infty} f_2(\eta)$ is indeed equal to the value given in (63). The other conditions are $f_2 = df_2/d\eta = \theta_2 = 0$ at $\eta = 0$, $\theta_2(\infty) = 0$. Upon integration we find for (63)

$$\lim_{\eta \rightarrow \infty} f_2(\eta) = 0.086931 \eta^3 - 0.17579 \eta^2 + 0.47750 \eta + \text{terms of order lower } \eta. \tag{66}$$

Matching for F_2 now gives

$$F_2(0) = -0.27605; \quad \left. \frac{dF_2}{d\xi} \right|_{\xi=0} = 0.47750. \tag{67}$$

With (29) and (67) equation (62) can be integrated.

numerical results

For subsequent use some important numerical data are collected in table 1. These figures are related to the skin friction, heat transfer and the mass flow through the boundary layer.

TABLE 1

| i | $\left. \frac{d^2 f_i}{d\eta^2} \right _{\eta=0}$ | $\left. \frac{d\theta_i}{d\eta} \right _{\eta=0}$ | $F_i(\infty)$ |
|---|---|---|---------------|
| 0 | 0.824516 | -0.710989 | 0.429209 |
| 1 | -0.306698 | 0.186442 | 0.021623 |
| 2 | 0.224248 | -0.067251 | 0.071661 |

It is furthermore necessary to give the graphs representing the various perturbations of the inner- and outer expansions (Figs. 3, 4, 5). As will be

shown later it is possible to construct over-all velocity- and temperature profiles with these graphs.

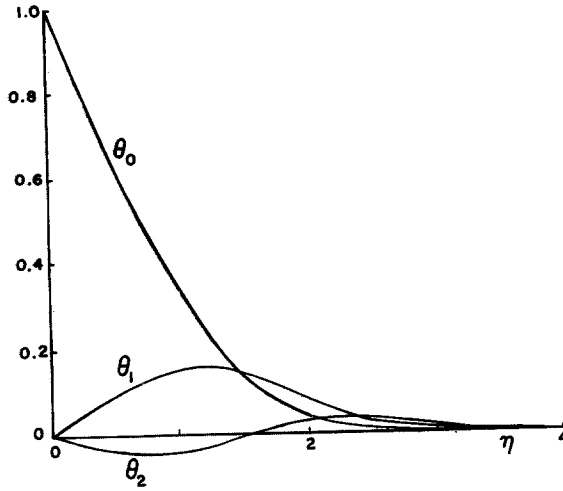


Fig.3 Temperature perturbations of inner expansion

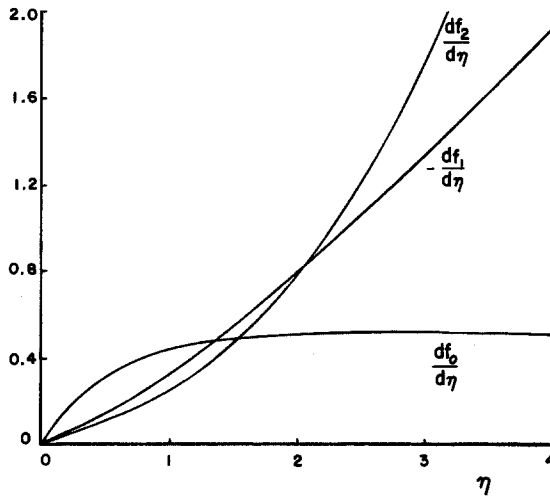


Fig.4 Velocity perturbations of inner expansion

5. Results

As considerable effort has been expended already in the past to investigate large Prandtl number free convection it is imperative to compare our results with those of the earlier studies. As being fit for comparison we see in the first place the work of Ostrach [3] and Le Fevre [1]. Ostrach presents exact numerical results by direct integration of the equations (4) and (5) for some special large Prandtl numbers. Le Fevre's analysis leads to an interpolation formula which joins both ends of the Prandtl number scale for which he had found exact data. This interpolation formula is satisfactorily compatible with the results of Ostrach (three decimal places) Other less accurate results will also be used for comparison.

The justification of the presentation of our method can be found by con-

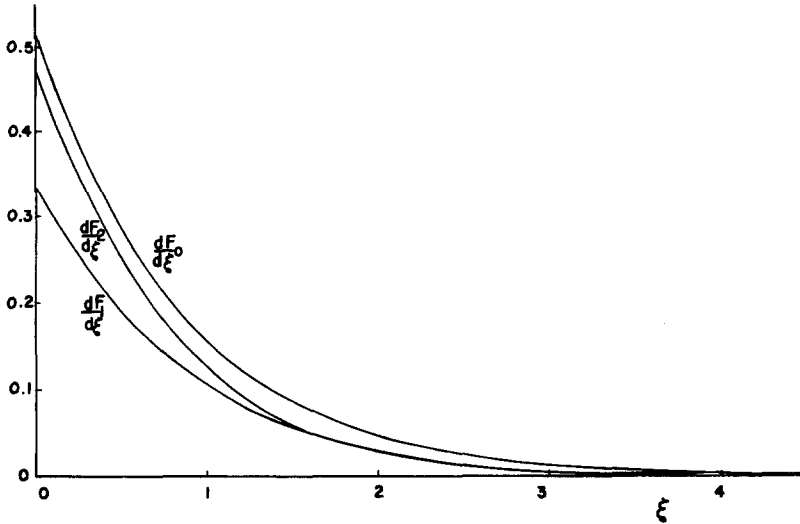


Fig.5 Velocity perturbations of outer expansion

sidering that the present results are drawn from equations which are of a balanced nature. This is contrary to the results of Ostrach which have been obtained by integration of equations containing the large parameter σ . This may be inconvenient from a numerical point of view. Our exact calculations, however, show that Ostrach's results are significant in all decimal places presented by him.

heat transfer

Let us first consider heat transfer with the well-known Nusselt-Grashof group (see [3])

$$\frac{Nu_x}{(Gr_x)^{\frac{1}{4}}} = - 2^{-\frac{1}{2}} \left. \frac{dh}{d\mu} \right|_{\mu=0} \quad (68)$$

As $\mu=0$ refers to the inner region we have to use (8) and (9) for obtaining

$$\frac{Nu_x}{(Gr_x)^{\frac{1}{4}}} = - 2^{-\frac{1}{2}} \sigma^{\frac{1}{4}} \left[\left. \frac{d\theta_0}{d\eta} \right|_{\eta=0} + \left. \frac{d\theta_1}{d\eta} \right|_{\eta=0} \sigma^{-\frac{1}{2}} + \left. \frac{d\theta_2}{d\eta} \right|_{\eta=0} \sigma^{-1} + O(\sigma^{-\frac{3}{2}}) \right] \quad (69)$$

which upon insertion of the figures of table 1 becomes

$$\frac{Nu_x}{(\sigma Gr_x)^{\frac{1}{4}}} = 0.50275 - 0.1318 \sigma^{-\frac{1}{2}} + 0.0475 \sigma^{-1} + O(\sigma^{-\frac{3}{2}}). \quad (70)$$

In table 2 the results of different analyses are given for $Nu_x/(\sigma Gr_x)^{\frac{1}{4}}$. It follows quite clearly from table 2 that for $\sigma=100$ and $\sigma=1000$ the present analysis and that of Ostrach lead to figures differing but one unit of the fourth decimal. Apparently the figures of Ostrach - including the other values of σ considered by him - are correct to four decimal places. From this we may directly infer by making use of the figures for $\sigma=1, 2$ and 10 that the truncation error in (70) is

$$\sim - 0.02 \sigma^{-\frac{3}{2}}. \quad (71)$$

TABLE 2

$Nu_x / (\sigma Gr_x)^{1/4}$ for various Prandtl numbers

| | present | Ostrach [3] | Le Fevre [1] | Brindley [10] |
|------|---------|-------------|--------------|---------------|
| 1000 | 0.49863 | 0.4987 | 0.499 | 0.4953 |
| 100 | 0.49004 | 0.4899 | 0.490 | 0.5244 |
| 10 | 0.4658 | 0.4650 | 0.465 | 0.5171 |
| 2 | 0.4333 | 0.4260 | 0.426 | |
| 1 | 0.4185 | 0.4010 | 0.401 | |

As a consequence formula (70) yields figures which for $\sigma > 100$ can at most differ in two units of the fifth decimal from the exact values. This accuracy can be guaranteed since the figures of table 1 are sufficiently accurate.

The solution of Le Fevre and ours have in common that they display the Prandtl number explicitly. As the figures of Le Fevre are correct in three decimal places the present solution must only be used for the calculation of heat transfer if it leads to more accurate results. From the truncation error (71) we may deduce that equation (70) produces figures which are accurate in four decimal places if $\sigma > 35$.

total mass flow

As the total mass flow is related to the complete boundary layer we have to use the results of the outer problem for its description. From (27) and table 1 we can derive for the total mass flow

$$\lim_{y \rightarrow \infty} \psi_{\text{outer}} = 4 \nu c x^{3/4} \sigma^{-1/4} \lim_{\xi \rightarrow \infty} F(\xi) = 4 \nu c x^{3/4} \sigma^{-1/4} \left[0.42921 + 0.02162 \sigma^{-1/2} + 0.07166 \sigma^{-1} + O(\sigma^{-3/2}) \right]. \quad (72)$$

If σ tends to infinity due to variations of k, ρ or c_p the total mass flow evidently will go to zero. Since the viscosity occurs also outside σ in (72) we have to expect a different result for $\nu \rightarrow \infty$. Using (3) it can be proved that the total mass flow is proportional to $\nu^{1/4}$ if σ is large enough.

By means of the inner expansion it is easily shown that the skin friction in large Prandtl number fluids is also proportional to $\nu^{1/4}$.

temperature- and velocity profiles

Another question of interest concerns the temperature- and velocity profiles. In constructing these profiles with the results of our analysis we have to make use of the so-called composite expansion technique which is one of the topics of matched asymptotic expansions. If we direct our attention first to the velocity distribution we find as the composite expansion using three term inner and outer expansions [13].

$$\frac{dg}{d\mu} = \sigma^{-1/2} \frac{\left(\frac{df_0}{d\eta} + \frac{df_1}{d\eta} \sigma^{-1/2} + \frac{df_2}{d\eta} \sigma^{-1} \right) \left(\frac{dF_0}{d\xi} + \frac{dF_1}{d\xi} \sigma^{-1/2} + \frac{dF_2}{d\xi} \sigma^{-1} \right)}{b_{10} + 2b_{20}\xi + 3b_{30}\xi^2 + (b_{11} + 2b_{21}\xi) \sigma^{-1/2} + b_{12}\sigma^{-1}} + O(\sigma^{-2}). \quad (73)$$

On account of the fact that the outer expansion for the temperature is exactly equal to zero the composite expansion coincides with the inner expansion

$$h(\mu) = \theta_0(\eta) + \theta_1(\eta)\sigma^{-\frac{1}{2}} + \theta_2(\eta)\sigma^{-1} + O(\sigma^{-\frac{3}{2}}). \tag{74}$$

If we want to compare (73) and (74) graphically with the profiles of Ostrach we have to resort to Prandtl numbers which are not too large, since for large σ the differences are graphically indistinguishable. The figures 6 and 7

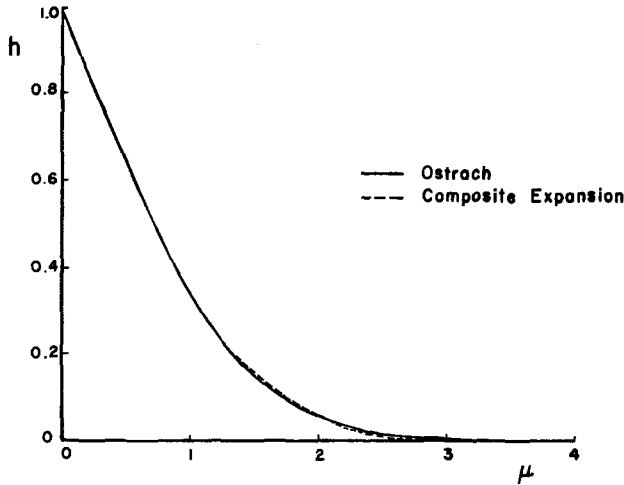


Fig.6 Comparison of temperature profiles (Ostrach and present) for $\sigma = 2$

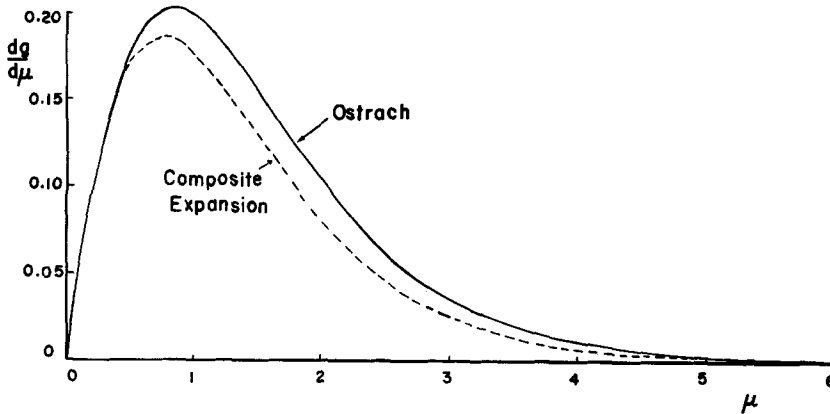


Fig.7 Comparison of velocity profiles (Ostrach and present) for $\sigma = 2$

show graphs for the velocity and the temperature for $\sigma=2$. It is seen that in the inner region the accuracy is greater than in the outer region. From the velocity this is directly evident. For the temperature profiles this may be concluded from the fact that only in the matching area a difference between Ostrach's result and ours can be seen. In order to illustrate the improved accuracy for larger values of σ velocity profiles are presented for $\sigma=10$ in Figure 8.

6. Concluding remarks

It may have become clear that the primary importance of the present study is a qualitative one. It has been attempted starting with physical considerations to expose the dual character of a large Prandtl number boundary layer of free convection through using those mathematical tools which are most suitable for the description of this problem. In particular, the role

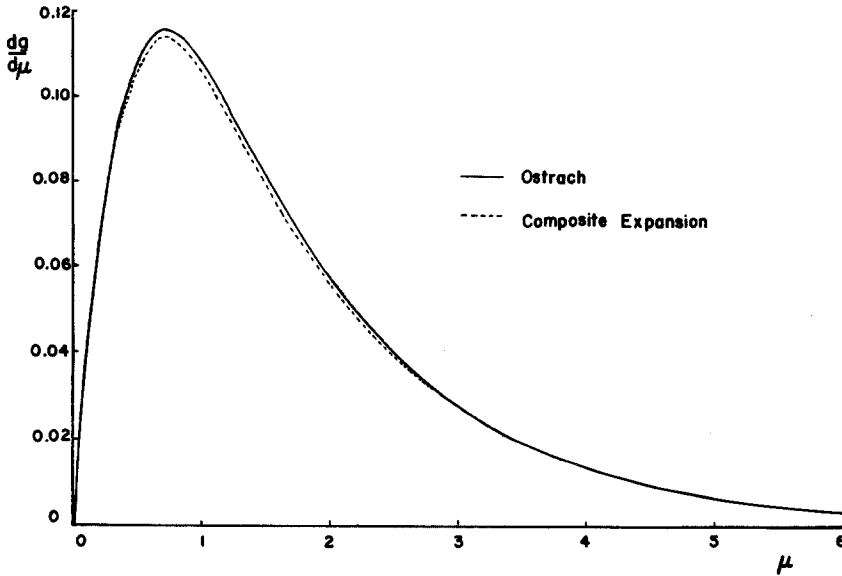


Fig.8 Comparison of velocity profiles (Ostrach and present) for $\sigma = 10$

of the outer region became obvious in this way.

A question still to be discussed concerns the expansion parameter in the expressions (70) and (72). One might wonder whether a physical explanation exists for this parameter being $\sigma^{-\frac{1}{2}}$. As an explanation we may give that these expansions are generated through matching of two regions. The ratio of the thicknesses of these regions is proportional to $\sigma^{-\frac{1}{2}}$ as may be shown through comparison of the inner variable η and the outer variable ξ . The rate of interaction of inner and outer region, as expressed by the matching technique, is proportional to the ratio of the thicknesses of the layers.

REFERENCES

1. E.J. Le FEVRE, Laminar free convection from a vertical plane surface, Ninth Intern. Congr. Appl. Mech., Brussels, paper I 168, Vol.4, 168-173 (1956).
2. H.SCHUH, Boundary layers of temperature, Resp. and Trans. 1007, AVA Monographs, British M.A.P. (1948).
3. S.OSTRACH, An analysis of laminar free-convection flow and heat transfer about a flat plate parallel to the direction of the generating body force. N.A.C.A. 1111 (1953).
4. H.K.KUIKEN, Perturbation techniques in free convection. Doctoral Thesis, Techn. Univ. Delft (1967).
5. P.S.LYKOUKIDIS, Natural convection of an electrically conducting fluid in the presence of a magnetic field. Int. J. Heat Mass Transfer 5, 23-34 (1962).
6. R.NARASIMHA and S.S.VASANTHA, Laminar boundary layer on a flat plate at high Prandtl number. Z.A.M.P. 17, 585-592 (1966).
7. G.W.MORGAN and W.H.WARNER, On heat transfer in laminar boundary layers at high Prandtl number. J. Aeronaut. Sci. 23, 937-948 (1956).
8. D.MEKSYN, New methods in laminar boundary layer theory. Pergamon Press (1961).
9. H.J.MERK, Rapid calculations for boundary-layer transfer using wedge solutions and asymptotic expansions. J. Fluid Mech. 5, 460-480 (1959).
10. J.BRINDLEY, An approximation technique for natural convection in a boundary layer. Int. J. Heat Mass Transfer 6, 1035-1048 (1963).
11. W.H.BRAUN and J.E.HEIGHWAY, An integral method for natural-convection flows at high and low Prandtl numbers. N.A.S.A. T.N. D-292 (1960).
12. L.PRANDTL, Über Flüssigkeiten bei sehr kleiner Reibung. Verhandl. III. Int. Math. Kongr., Heidelberg, 484-491 (1904).

13. M. VAN DYKE, Perturbation techniques in fluid mechanics, Academic Press (1964).
14. H. SCHLICHTING, Grenzschichttheorie. Verlag G. Braun (1964).
15. H. K. KUIKEN, Boundary layer conditions in free convection, J. Eng. Math. 2, 95-105 (1968).

[Received June 5, 1968]